

Femtosecond dynamics of CdTe quantum dots in water

Mikel Sanz^a, Miguel A. Correa-Duarte^b, Luis M. Liz-Marzán^b, Abderrazzak Douhal^{a,*}

^a *Departamento de Química Física, Sección de Químicas, Facultad de Ciencias del Medio Ambiente, Universidad de Castilla-La Mancha, Avda. Carlos III, S.N. 45071 Toledo, Spain*

^b *Departamento de Química Física and Unidad Asociada CSIC-Universidade de Vigo, 36310 Vigo, Spain*

Received 27 April 2007; received in revised form 10 October 2007; accepted 13 November 2007

Available online 21 November 2007

Abstract

We present studies on femtosecond to nanosecond fluorescence dynamics of aqueous solutions of cadmium telluride (CdTe) quantum dots (QDs) with diameters of 3.1 and 3.6 nm. Ultrafast times in the range 200–320 fs and 1.6 ps were determined, and assigned to electron relaxation to the bottom of the conduction band and to recombination of trapped electrons and holes. These times are common to the relaxation mechanisms of QDs in solution, and therefore suggests that intrinsic mechanisms for electron and hole relaxation dominate over surface effects, in agreement with other reports. Additionally, times of ~40 ps, ~600 ps and ~20 ns due to radiative transitions were recorded. These results are relevant to understanding the photodynamics of CdTe and other QDs in water which should play a fundamental role in their signal when used in biological media.

© 2007 Elsevier B.V. All rights reserved.

Keywords: Femtosecond; Cadmium telluride; Quantum dots; Fluorescence; Ultrafast dynamics; Electron; Holes; Relaxation; Recombination

1. Introduction

Within the last two decades, the interest in semiconductor quantum dots (QDs) has increased rapidly [1]. The physical and chemical properties of semiconductor QDs differ from those of the bulk materials. Due to quantum size effects, the bandgap energy can be tuned and the formation of atomic like levels occurs at the edges of the bandgap [2]. Therefore, many properties of these materials can be systematically described and understood in terms of quantum confinement effects [3–6]. These special properties have turned semiconductor nanocrystals into promising materials for many potential technological applications [7–12].

Though the basic properties of II–VI nanocrystals including electron–hole energy states and optical transition probabilities are well established and understood [13–15], there are a number of important issues relevant to primary photophysical and photochemical processes that require further studies. Photoluminescence properties of nanocrystals typically depend on surface structure, chemical environment, migration of carriers and a

number of interactions [16]. An understanding of these properties beyond simplified quantum dot considerations is necessary for establishing photoluminescence mechanisms and developing highly efficient light-emitting nanocrystalline devices or solar cells.

Unlike nanocrystals of CdS and CdSe, whose structural and luminescence properties, as well as their surface-related emission, have been examined in detail [2,17–21] considerably less attention has been paid to cadmium telluride (CdTe) nanocrystals. Several groups have performed the synthesis of CdTe nanocrystals in various environments, showing that thiol-capped CdTe QDs are some of the most robust and highly fluorescent nanoparticle materials synthesized in aqueous medium and in other solvents [22–29]. However, the study of their ultrafast luminescence properties is still in an early stage [27–32].

Recent studies of CdTe nanoparticles in the fs-regime have been carried out in chloroform [30], using CdSe/CdTe tetrapods [30,31] and CdTe/CdSe core–shell quantum dots in toluene [32]. At the best of our knowledge, there is no report on the fs-regime of CdTe nanoparticles in aqueous solutions.

Unlike femtosecond transient absorption or pump–probe laser spectroscopies, fluorescence up-conversion is unique in its ability to probe the excited state without interference from

* Corresponding author. Fax: +34 925 268840.

E-mail address: Abderrazzak.douhal@uclm.es (A. Douhal).

other processes such as excited-state absorption or ground-state recovery.

In this paper, we report on studies of time-resolved photoluminescence transients of thioglycolic acid-capped CdTe nanoparticles in a neutral aqueous solution. The obtained results show a rich dynamics with transient times ranging from 200 fs up to 20 ns. We discuss the nature of the related events and propose an energetic scheme for these excited QDs in water.

2. Experimental

Thioglycolic acid-stabilized (TGA) CdTe QDs were synthesized as described elsewhere [16]. The duration of the heat treatment was 1.5 h for sample 1 and 20 h for sample 2, resulting in CdTe QDs with average diameters of approximately 3 and 3.6 nm for samples 1 and 2, respectively, as determined by high-resolution transmission electron microscopy (HRTEM). Prior to the measurements, the samples were diluted by adding an aliquot of a stable and concentrated aqueous solution of CdTe to neutral water (Mili-Q) and D₂O (Aldrich, 99.9%).

Taking into account the following equation: $D = (9.8127 \times 10^{-7})\lambda^3 - (1.7147 \times 10^{-3})\lambda^2 + ((1.0064)\lambda - 194.84)$ [33] where D (nm) is the diameter of the nanocrystal sample, and λ (nm) is the wavelength of the first excitonic absorption peak of the corresponding sample, we calculated the average values of nanoparticle size. The reported function provided fitting functions of the experimental data which are valid from a nanocrystal size range of 3–8 nm. We obtained diameters of 3.1 and 3.6 nm for the QDs with the excitonic first peak of 543 and 588 nm, respectively, a very similar result to that determined by HRTEM.

The UV–vis absorption and emission spectra were recorded on Varian (Cary E1) and PerkinElmer (LS-50B) spectrophotometers, respectively. Picosecond time-resolved emission decays were obtained using a time-correlated single-photon counting spectrophotometer (FluoTime 200, Picoquant) described earlier [34]. The excitation was performed at 371 nm and the emission was detected at magic angle. The instrumental response function (IRF) was typically 65 ps. Time-resolved emission transients were observed by using the fluorescence up-conversion technique [35]. Briefly, the system consists of a femtosecond (fs) Ti:sapphire oscillator (Tissa 100, CDP) pumped with a 5-W diode laser (Verdi 5, Coherent). The pulses (60 fs, 450 mW) were centred on 736 nm at 82 MHz repetition rate. The light beam was doubled in 1-mm BBO crystal and a dichroic mirror was used to separate the fundamental from the doubled beam (368 nm) sent for sample excitation. Typically, the energy of the excitation pulse at the sample was ~ 0.5 nJ. The remaining fundamental light was used to gate the emission of the sample flowing in a 1-mm quartz-rotating cell. The emission was collected and focused into a 0.3-mm BBO crystal (type I) using reflective optics. The gating pulse was time delayed and focused into the nonlinear crystal to overlap with the sample fluorescence. The resulting up-converted signal in the UV region was filtered, entered to a double monochromator and detected with a photomultiplier tube. The IRF of the apparatus measured by gating the Raman signal from solvent is 170 fs for a 1-mm sample cell. The data were deconvoluted with the IRF signal of

the apparatus and fitted to a multi-exponential function using the FluoFit package. The quality of the fits was characterized in terms of residual distribution and reduced χ^2 values. All experiments were carried out at 293 ± 1 K.

3. Results and discussion

3.1. Steady-state and ps-resolved observation

The quantum yield of CdTe nanocrystals is directly related to the used TGA/Cd ratio. Our particles were synthesized following a previous procedure and using the same chemical precursors, capping agent (TGA: size of the thioglycolic acid ligand ~ 0.47 nm) and solvent (water) [36]. Therefore, our particles prepared with a TAG/Cd ratio of 2 should have a quantum yield of 15%, which also agrees with the 13.6% reported earlier for CdTe QDs using the same TGA/Cd ratio [37].

Fig. 1 shows a TEM micrograph of the ~ 3.6 nm diameter CdTe QDs, while Fig. 2 gives the absorption and photoluminescence spectra of both CdTe particles having diameters of 3.1 and 3.6 nm. The absorption spectra indicate that CdTe nanoparticles have a wide range of absorption. Emission spectra (characterized by Gaussian lineshape and relatively narrow spectral width, FWHM ~ 190 meV) show only a band-edge fluorescence peak, which is slightly red-shifted from the absorption onset (global Stokes shift ~ 1.6 eV) indicating that surface defects, rather than lattice defects, must be responsible for trapping the exciton. The same behaviour was observed for TGA, mercaptopropionic acid (MPA) [26] and TOP/DDA (trioctylphosphine/dodecylamine) capped CdTe QDs upon transfer into water [28].

Our emission spectra exhibit the band-edge emission. In a previous work, its presence has been explained by invoking different recombination mechanisms, such as recombination of the delocalized electron–hole (e–h) pairs strongly coupled to

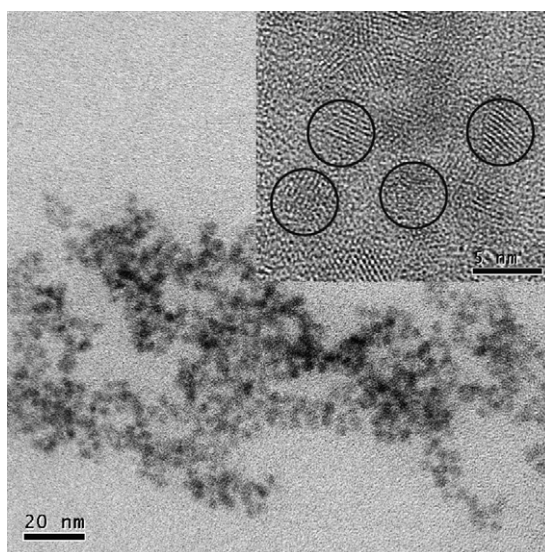


Fig. 1. TEM micrographs of 3.6 nm in diameter CdTe quantum dots (QDs). The inset shows a high-resolution image demonstrating good crystallinity of the single QDs. In order to improve the contrast on the TEM microscope, the samples were washed with isopropanol and redispersed in a water/DMF (1:100) solution.

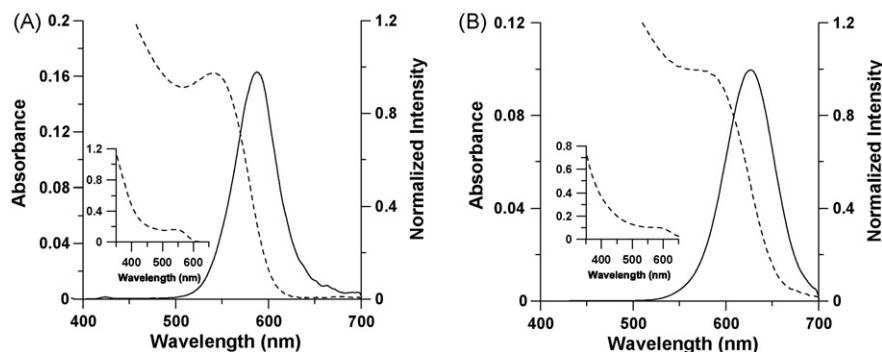


Fig. 2. Room temperature UV–vis (dashed line) absorption and emission (solid line) spectra of a neutral aqueous solution of CdTe nanoparticles of (A) 3.1 nm and (B) 3.6 nm diameter. The insets show the entire absorption spectra. For emission, the excitation wavelength was 370 nm for both samples.

lattice vibrations or recombination through localized states, possibly originating from surface effects [38]. The predominance of band-edge fluorescence (due to exciton radiative recombination) over the fluorescence from deep-trap states (IR-band, not observed) indicates a low density of deep-trap states, most likely due to the nature of the surface capping agent, opposite to what has been reported for CdTe QDs in glasses [39]. The intensity maxima of absorption and emission bands are shifted toward shorter wavelengths when the QD size is decreased. This result is a consequence of quantum size confinement, and the shifts for H₂O and D₂O solutions are similar. The excitonic absorption peaks are centred at 543 and 588 nm for 3.1 and 3.6 nm diameter nanoparticles, respectively. The emission peaks (586 and 634 nm) are shifted (relative to the absorption) by 170 and 155 meV (~ 1350 and 1236 cm⁻¹), respectively. These global Stokes shifts are explained either in terms of strong electron–phonon interaction or by the presence of localized states (surface and/or defect) involved in the band-edge emission [40].

To compare the ps-dynamics for both sizes of QDs, we will focus on emission at wavelengths approximately corresponding to the excitonic absorption peak (540 and 580 nm for 3.1 and 3.6 nm size QDs, respectively) and to the emission maxima for both QD sizes (580 and 630 nm for 3.1 and 3.6 nm QDs, respectively). We performed ps–ns lifetime measurements for both QDs in water at different wavelengths of observation. The ps-decays (not shown) were fitted using a multi-exponential function ($I = \sum_i a_i \exp(-t/\tau_i)$) through which we obtained three

decaying components having times in the ps and ns regimes. Table 1 gives the corresponding data.

Prior to the discussion of our results, we recall that a previous report [27] has suggested the existence of two kinds of nanoparticles for thiol-capped CdTe QDs in water: one type displays surface traps due to incomplete capping, while the other shows almost perfect surface and therefore only exciton luminescence. The observed emission decays in the thiol-capped CdTe QDs in water are not single exponentials, and 2- and 3-exponential models failed to yield an accurate fit to the experimental signal [27]. However, recent ps-experiments on TOP/DDA (trioctylphosphine/dodecylamine) capped CdTe QDs and transferred into water by the use of aminoethanethiol-HCl (AET) or MPA reported a single exponential emission decay (~ 20 ns) assigned to excitonic luminescence from a nearly perfect surface [28,29]. These previous works also show the effect of both solvent and capping material on the emission decays.

Very recently, a report on luminescence properties of thiol-capped CdTe QDs in water shows that an increase in particle size drastically reduces the short component and a single-exponential decay yielding a fluorescence lifetime of 145 ns has been recorded for MPA-capped CdTe QDs (diameter ~ 6 nm) [26]. This observation is explained in terms of stabilized Te-related traps relative to the valence band position of the CdTe nanoparticle, a result supporting the model proposing that the luminescence properties are strongly influenced by the surface quality and reflecting conditions of Oswald ripening growth.

Table 1

Values of time constants (τ_i) and normalized (to 100) pre-exponential factors (a_i) from the multi-exponential fitting function ($I = \sum_i a_i \exp(-t/\tau_i)$) of the ps–ns emission decays of CdTe nanoparticles in water at different wavelengths of observation

QD diameter (nm)	λ (nm)	τ_1 (ps)	a_1 (%)	τ_2 (ps)	a_2 (%)	τ_3 (ns)	a_3 (%)
3.1	500	40	70	575	15	17.9	15
	540	41	38	485	14	21.2	48
	580	37	49	550	13	21.1	38
	620	40	44	545	15	22.0	41
3.6	540	50	64	725	17	15.2	19
	580	44	37	650	20	16.8	43
	600	47	39	830	19	17.3	42
	630	48	45	710	14	17.5	41

Here (Table 1), we observed multi-exponential decays for the TGA-capped CdTe QDs. The shortest component ($\tau_1 = 40 \pm 10$ ps for 3.1 nm and 45 ± 10 ps for 3.6 nm nanoparticles) is assigned to radiative depopulation due to band-edge recombination or to e–h recombination at the surface [41]. The contribution of this decay is larger at shorter wavelengths, being the most important process among “radiative” transitions (see pre-exponential factors in Table 1). This result, in addition to the small influence of particle size on the decay time value, suggests that the principal process for this decay is the band-edge recombination, enhanced by a higher energy of the Te-related traps with respect to the valence band position of CdTe [26].

The 485–850 ps component (τ_2), assigned to radiative electron–hole (e–h) recombination processes due to surface defects, becomes larger with the diameter of nanoparticles. It changes from 535 ± 50 ps for 3.1 nm to 740 ± 90 ps for 3.6 nm. In both cases, the contribution of e–h recombination in the ps–ns signal is weak (Table 1). The value of the ns-component (τ_3) is similar to that reported in previous works [26,28]. Its contribution to the signal is significant and it increases with the observation wavelength. However, the value of τ_3 decreases from 21 ± 2 down to 17 ± 2 ns with increasing particle size from 3.1 to 3.6 nm. This result agrees with that observed using different capping agents, such as TOP/DDA [28]. However, it does not agree with the report on thiol-capped CdTe, which shows an increase in the ns lifetime with the size of the particle, and where longer lifetimes, up to 145 ns, have been observed [26]. These differences reflect the effect of a small experimental-condition change (fluctuation) in the preparation of larger nanoparticles, and which controls thermodynamics and kinetics of growth. In our case, rate constants of non-radiative processes due to deep traps increase with the size of the QDs, leading to a decrease of component lifetimes as we actually observe.

To check the possible influence of the H-bonding network of water on the decay times, we carried out the same experi-

ments using deuterated water, observing no significant changes in both absorption and emission spectra, as well as in the ps-decay times using non-H-bonding solvents. A few points should be addressed here. First: in D₂O there is no aggregation of CdTe nanoparticles. Second, possible H-bonding interactions between water molecules and CdTe or the capping material should be very fast, and may reshape the NPs surface. Thus, the adsorbed layers of water molecules at the surface of the particles may affect the whole relaxation dynamics which may involve the dynamics of the water H-bond network. The H/D isotope exchange may affect the global dynamics of water. Therefore, water interactions should reshape the surface of the QDs affecting the non-radiative e–h recombination at surface defects. On the other hand, surface passivation due to the different interactions of capping molecules with the environment might lead to relaxed surfaces, and therefore to longer lifetimes, which seems to happen in D₂O, where the value of ns lifetime increases. For the 3.6-nm nanoparticles, the value of τ_3 changes from 17 ± 1 ns in H₂O to 21 ± 1 ns in D₂O, while we observed no change in the other decay times (see supplement material). The present result provides experimental evidence for the importance of H-bonding interactions between water and the capping material on the surface structure and emission decay times of CdTe QDs. The increase in the fluorescence lifetime in D₂O suggests a surface passivation of the QDs, decreasing the non-radiative e–h recombination rate at surface defects.

3.2. Femtosecond observation

To obtain information on the first events after excitation, we gated the emission at the femtosecond (fs) time scale and at different wavelengths of observation. Fig. 3 shows the obtained fs-transients of CdTe nanoparticles for both sizes. Fig. 4 exhibits a comparison of the transients at wavelengths corresponding to (A) 540 and 580 nm for 3.1 and 3.6 nm QDs, and (B) 580 and

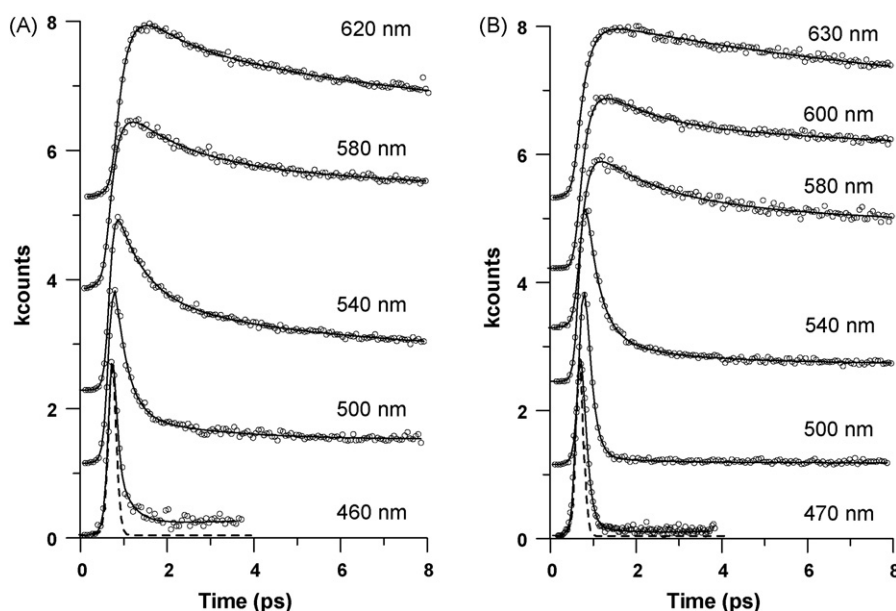


Fig. 3. Femtosecond-emission transients of (A) 3.1 nm and (B) 3.6 nm CdTe nanoparticles at different observation wavelengths. The solid lines correspond to the best fitting multi-exponential functions. The dashed peak is the IRF (170 fs).

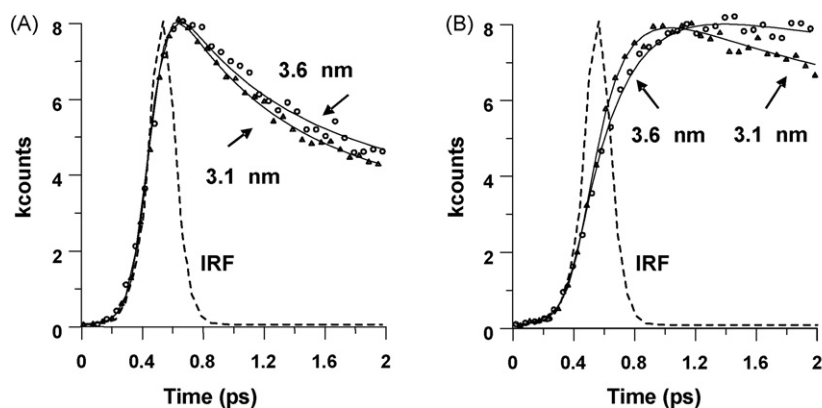


Fig. 4. Femtosecond-emission transients of (A) the excitonic absorption peak and (B) the maximum of the emission spectrum of CdTe NPs in water for (○) 3.1 and (△) 3.6 nm at different representative observation wavelengths. The solid lines are from the best fit using multi-exponential functions and the dashed peak is the IRF (170 fs).

Table 2

Values of time constants (τ_i) and normalized (to 100) pre-exponential factors (a_i) from the multi-exponential fitting function of the fs-emission transients of CdTe nanoparticles in water at different observation wavelengths

QD diameter (nm)	λ (nm)	τ_1 (fs)	a_1 (%)	τ_2 (ps)	a_2 (%)	τ_3 (ps)	a_3 (%)
3.1	460	180	93	1.6	7		
	500	210	81	1.7	13	40*	6
	540	200	34	1.5	43	41*	23
	580	220	-47	1.7	37	37*	16
	620	240	-47	1.5	29	40*	24
3.6	470	200	99	1.6	1		
	500	190	98	1.8	2		
	540	240	87	1.6	7	50*	6
	580	220	48	1.7	19	44*	33
	600	315	-49	1.6	25	47*	26
	630	320	-51	1.6	27	48*	22

The sign (-) before the values of a_i indicates a rising component in the transient. The (*) indicates a value measured in the ps–ns apparatus and fixed when fitting fs-transients.

630 nm for 3.1 and 3.6 nm QDs, respectively. Table 2 displays the values of the times (τ_i) and corresponding normalized (to 100) pre-exponential factors (a_i) of the fitting exponential functions ($I = \sum_i a_i \exp(-t/\tau_i)$). The 50-ps time constant obtained from the ps-measurements was fixed in the fit of the signal at this short-time window. The two other components have times of 200–300 fs and 1.6 ps.

Since the band gap for CdTe nanoparticles of these sizes in water is ~ 2 eV [42] ($\sim 16,132$ cm $^{-1}$) and our excitation carries 3.37 eV ($\sim 27,147$ cm $^{-1}$, 368 nm), the excess of excitation energy is about 1.37 eV ($\sim 11,042$ cm $^{-1}$) (Fig. 5). The absence of a rising component in the signal at the short wavelengths of observation suggests that the time necessary for an excited electron to relax to the excitonic level (process 1nr in Fig. 5) is shorter than 50 fs (our time resolution). In a previous study on CdSe QDs, the population of electron states is almost completely established within the time scale of the pump pulse duration [43]. At the excitonic band, we observed a strong radiative emission (band-edge luminescence).

In the following, we analyse the trend and shape of the transients and related times. The behaviour of the signals can be divided into two categories reflecting two regions. Category I corresponds to the range of short wavelengths up to ~ 540

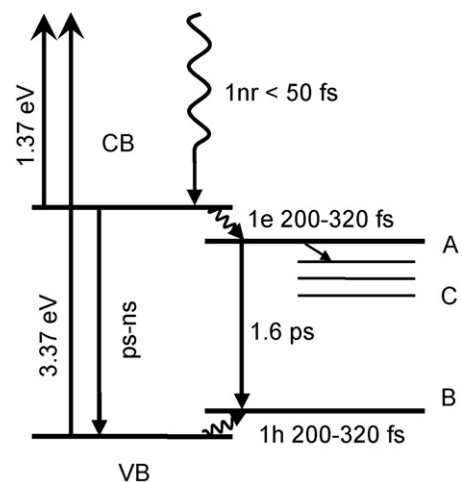


Fig. 5. Schematic illustration of the energetic, electronic and related transitions involved in CdTe QDs in water upon fs-excitation. VB: valence band; CB: conduction band. For the nomenclature of the transitions (1nr, 1e and 1h) see text for details.

(for 3.1 nm QDs) and ~ 580 nm (for 3.6 nm QDs), and where we observed fast decays (τ_1) of approximately 200 ± 50 fs, and 1.6 ± 0.2 ps. Category II involves wavelengths longer than ~ 540 and ~ 580 nm (for 3.1 and 3.6 nm QDs, respectively), and at which we observed a rising component of a similar fs-time, and a decaying component with a time of 1.6 ps. Clearly, the decaying and rising fs-component is of a common channel connecting both regions. It involves ultrafast events leading to the formation of trapped excited and hot electrons (at the conduction band) or to non-radiative relaxation of hot electrons and holes (1e and 1h in Fig. 5, respectively). The path followed by electrons through the conduction band and the jump of holes through the valence band can be easily seen from transients recorded at different wavelengths that show a progressive increase in the rise-time (τ_1) with increasing the detection wavelength (Table 2). This value of the decay time in the rising component slightly increases with QD size (230 and 320 fs for 3.1 and 3.6 nm, respectively, Fig. 4B and Table 2). Therefore, the related ultrafast event becomes less fast when the surface/volume ratio decreases for smaller QDs. Note that the corresponding decay value can be affected by the auto-absorption of the emission that can take place at wavelengths shorter than that of the excitonic peak. At longer wavelengths of observation, such auto-absorption process cannot occur, and therefore, the observed value is safe from the above-described phenomenon. In addition to that, the behaviour of our transients is similar to that obtained for CdS nanoparticles in water [44]. In those experiments, the emission peak is sufficiently shifted with respect to the absorption band, so that auto-absorption of emission is almost absent. The obtained transients for the whole emission range showed trends similar to our transients. The same behaviour was observed in CdS nanoparticles in AOT/*n*-heptane reverse micelles [45]. Therefore, the observed 200 fs decaying component should not be significantly affected by the auto-absorption process at short wavelengths.

If we compare the obtained times with those for CdTe QDs in chloroform (a solvent largely different from water), characterized using fs time-resolved transient absorption spectroscopy [30], we find that they are not very different from our results in water. At 680 nm the signal presents a rise-time of about 300 fs and two decay components of 1.0 and 25 ps, approximately. Therefore, the ultrafast dynamics is not very sensitive to the nature of the solvent, suggesting an intrinsic origin for their mechanisms.

In the case of thiol-capped CdS QDs in water, the ultrafast dynamics has been studied using fluorescence up-conversion techniques [44]. They observed two different regions depending on the observation wavelength (just like here). In the first region – wavelengths shorter than 550 nm – they obtained two decay components of 1.0 and 10 ps. Whereas in the second region, around 650 nm, the transients present an initial rise-time of 1.0 ps and a decay component of ~ 10 ps. For all the transients, there is an additional component that could not be resolved in the gate of observation, 30 ps. Clearly, for CdS QDs the two shorter times are longer than those obtained for CdTe QDs in water, ~ 0.25 and 1.6 ps. Note that the obtained 1-ps time of the ultrafast component might be limited by the time resolution (not indicated the related work) of the apparatus [44]. Never-

theless, in the case of CdS QDs prepared within Aerosol-OT (AOT)/*n*-heptane reverse micelles (confining nanopool) containing water [45], with $W_0 = 4.5$ ($W_0 = [\text{H}_2\text{O}]/[\text{AOT}]$), the results are very similar to ours, obtaining times of 0.2 and 1.9 ps, for the fast decays, in the region of 530–580 nm. Thus, for both CdTe and CdS in water solution, short components having times of 200–300 fs and 1.5–2 ps are observed. They should reflect common ultrafast and intrinsic relaxation channels for electron and hole relaxation, and recombination. As far as we know, no fs-study has been carried out on CdSe NPs in water, probably due to their large photosensitivity of their luminescence properties [47]. Therefore, we cannot extend our comparison to these systems in water. Nevertheless, the ultrafast dynamics of CdSe in chloroform shows comparable fs and ps times [21], re-enforcing the idea that in the ultrashort regime, intrinsic mechanisms in NPs deactivation dominate over surface defects.

In other NP systems, the short ps-decay time ($\tau_2 = 1.6 \pm 0.2$ ps) has been assigned to Auger recombination [39], hole relaxation [46] or to recombination processes due to shallow traps [14]. In our case, the absence of a rise-time of this value in the longer wavelength region suggests that hole relaxation is produced only within hundreds of fs and not in the ps regime. The value of this fast time is approximately the same for both particle sizes, and does not depend on the gated region. However, the contribution (a_2) of this component to the signal changes with the size of the QDs as shown in Table 2 and Fig. 4. The estimated number of absorbed photons per one NP is one. We explain the decrease in the contribution upon increasing the QD size in terms of a reduction of the surface states acting as recombination centres. Larger CdTe nanoparticles have a smaller surface/volume ratio and therefore, a lower probability of the related recombination events to act at the surface states.

To explore whether Auger effect has significant contribution in this fast decay of our NPs, we studied the influence of pump fluence on the transients. We reduced the fluence from 0.5 to 0.065 nJ, being the latter the minimum value at which we could record a measurable signal. In the first case, and as said above the estimated number of photons per nanoparticle is practically one. We obtained no significant difference in the gated transients (not shown). This result suggests that under our normal experimental conditions, Auger effects are absent or insignificant. Pumping with higher excitation fluence (~ 1 nJ per pulse at 82 MHz) apparently leads to decomposition of the nanoparticles.

At the fs-regime, we observed no differences between the normal-water transients and those using deuterated water as solvent at “normal” pumping conditions (see supplement material). The result suggests that the possible H-bonding interactions of water with the capping TGA groups (strong H-bonding acceptor and donor sites) should be very fast (less than 50 fs). As said above, the ns-component becomes longer in D₂O (21 ns compared to 17 ns in water). Another possible explanation is that intrinsic mechanisms in radiative and non-radiative deactivation dominate over surface defects, as it is supported by the similarity of the ultrafast components in the relaxation of several NPs in solution: CdTe in water (present study) and in chloroform [30], and of CdS in water [44,45], and CdSe in chloroform [21].

Following the proposed schemes of electron relaxation dynamics in semiconductors [15,17,21,44,48], and using our results for CdTe in water, we thus propose the model shown in Fig. 5. Under our experimental conditions, an electron is deposited with an excess of energy into the conduction band by absorption of a photon, leaving a hole in the valence band (VB). The pumped electron (found with an energy excess of ~ 1.37 eV) relaxes in less than 50 fs to lower levels of the conduction band. Within 200–320 fs after the photoexcitation, the electron can quickly relax (1e) to the bottom of the conduction band (A) by intraband transition and, at the same time, the created hole can jump (1h) up to the top of the valence band (B). In 1.6 ps, the relaxed electron in A and jumped hole in B from shallow traps can recombine. In tens of ps to few ns, radiative depopulation due to band-edge recombination or to recombination of electrons at surface states is produced. Another possibility is that electrons can relax to a deep trap (C), from where they will recombine with holes within hundreds of ps. However, as we observed no IR band emission of this process, we do not invoke this phenomenon in CdTe QDs under our experimental conditions.

4. Conclusion

In this work, we have reported on fs–ps relaxation and dynamics of CdTe nanoparticles (3.1 and 3.6 nm in diameter) in neutral water. Ultrafast times in the range of 200–320 fs and 1.6 ps were determined, and assigned to electron relaxation to the bottom of the conduction band and to recombination of trapped electrons and holes; while times of ~ 40 ps, ~ 600 ps and ~ 20 ns due to radiative transitions were recorded. It comes out that times of 200–300 fs and 1.5–2 ps in the dynamics of NPs in water or in other solvents, are common, suggesting that intrinsic mechanisms of electron and hole relaxation dominate for the radiative and non-radiative deactivation pathways. We believe that these results might be important for a better understanding of nanoparticle photodynamics in biological media – for example detecting cancer – where water is the natural solvent, and for developing nano-biotechnology and other related fields.

Acknowledgements

This work was supported by the “Consejería de Educación y Ciencia” of JCCM and MEC through projects PBI-05-046 and CTQ2005-00114, and by the Consellería de Educación e Ordenación Universitaria (Xunta de Galicia). The authors are indebted to B. Rodríguez from CACTI (U. Vigo) for performing the TEM measurements.

Appendix A. Supplementary data

Supplementary data associated with this article can be found, in the online version, at doi:10.1016/j.jphotochem.2007.11.012.

References

- [1] A.P. Alivisatos, *Science* 271 (1996) 993.
- [2] L.E. Brus, *J. Chem. Phys.* 90 (1986) 2555.
- [3] H. Weller, *Angew. Chem. Int. Ed.* 32 (1993) 41.
- [4] S.V. Gaponenko, *Optical Properties of Semiconductor Nanocrystals*, Cambridge University Press, Cambridge, 1998.
- [5] U. Woggon, *Optical Properties of Semiconductor Quantum Dots*, Springer-Verlag, Berlin, 1996.
- [6] V.I. Klimov, A.A. Mikhailovsky, S. Xu, J.A. Hollingsworth, C.A. Leatherdale, H.J. Eisler, M.G. Bawendi, *Science* 290 (2000) 314.
- [7] M. Bruchez Jr., M. Moronne, P. Gin, S. Weiss, A.P. Alivisatos, *Science* 281 (1998) 2013.
- [8] W.C.W. Shan, S. Nie, *Science* 281 (1998) 2016.
- [9] M. Han, X. Gao, J.Z. Su, S. Nie, *Nat. Biotechnol.* 19 (2001) 631.
- [10] D. Gerion, F. Pinaud, S.C. Williams, W.J. Parak, D. Zanchet, S. Weiss, A.P. Alivisatos, *J. Phys. Chem. B* 105 (2001) 8861.
- [11] A.P. Alivisatos, *Nat. Biotechnol.* 22 (2004) 47.
- [12] A. Fu, W. Gu, B. Boussert, K. Koski, D. Gerion, L. Manna, M. Le Gros, C.A. Larabell, A.P. Alivisatos, *Nano Lett.* 7 (2007) 179.
- [13] M.G. Bawendi, M.L. Steigerwald, L.E. Brus, *Ann. Rev. Phys. Chem.* 41 (1990) 477.
- [14] V.I. Klimov, A.A. Mikhailovsky, D.W. McBranch, C.A. Leatherdale, M.G. Bawendi, *Phys. Rev. B* 61 (2000) R13349.
- [15] C. Burda, X.B. Chen, R. Narayanan, M.A. El-Sayed, *Chem. Rev.* 105 (2005) 1025.
- [16] M. Gao, S. Kirstein, H. Mohwald, A.L. Rogach, A. Kornowski, A. Eychmuller, H. Weller, *J. Phys. Chem. B* 102 (1998) 8360.
- [17] D.F. Underwood, T. Kippeny, S.J. Rosenthal, *J. Phys. Chem.* 105 (2001) 436.
- [18] S.F. Wuister, A. van Houselt, C.D. Donegá, D. Vanmaekelbergh, A. Meijerink, *Angew. Chem. Int. Ed.* 43 (2004) 3029.
- [19] C. Burda, M.A. El-Sayed, *Pure Appl. Chem.* 72 (2000) 165.
- [20] X. Wang, L. Qu, J. Zhang, X. Peng, M. Xiao, *Nano Lett.* 3 (2003) 1103.
- [21] H. Wang, C. de Mello Donegá, A. Meijerink, M. Glasbeck, *J. Phys. Chem. B* 110 (2006) 733.
- [22] N. Gaponik, D.V. Talapin, A.L. Rogach, K. Hoppe, E.V. Shevchenko, A. Kornowski, A. Eychmuller, H. Weller, *J. Phys. Chem. B* 106 (2002) 7177.
- [23] N. Gaponik, D.V. Talapin, A.L. Rogach, A. Eychmuller, H. Weller, *Nano Lett.* 2 (2002) 803.
- [24] C.B. Murray, D.J. Norris, M.G. Bawendi, *J. Am. Chem. Soc.* 115 (1993) 8706.
- [25] C. Schulz-Drost, V. Sgobba, D.M. Guldi, *J. Phys. Chem. C* 111 (2007) 9694.
- [26] A.L. Rogach, T. Franzl, T.A. Klar, J. Feldmann, N. Gaponik, V. Lesnyak, A. Shavel, A. Eychmuller, Y.P. Rakovich, J.F. Donegan, *J. Phys. Chem. C* 111 (2007) 14628–14637.
- [27] A.M. Kapitonov, A.P. Stupak, S.V. Gaponenko, E.P. Petrov, A.L. Rogach, A. Eychmuller, *J. Phys. Chem. B* 103 (1999) 10109.
- [28] S.F. Wuister, L. Swart, F. van Driel, S.G. Hickey, C. de Mello Donegá, *Nano Lett.* 3 (2003) 503.
- [29] S.F. Wuister, C. de Mello Donegá, A. Meijerink, *J. Am. Chem. Soc.* 126 (2004) 10327.
- [30] S. Malkmus, S. Kudera, L. Manna, W.J. Parak, M. Braun, *J. Phys. Chem. B* 110 (2006) 17334.
- [31] P. Peng, D.J. Miron, S.M. Hughes, J.C. Johnson, A.P. Alivisatos, R.J. Saykally, *Nano Lett.* 5 (2005) 1809.
- [32] P.T. Chou, C.Y. Chen, C.T. Cheng, S.C. Pu, K.C. Wu, Y.M. Cheng, C.W. Lai, Y.H. Chou, H.T. Chiu, *Chem. Phys. Chem.* 7 (2006) 222.
- [33] W.W. Yu, Y.A. Wang, X.G. Peng, *Chem. Mater.* 15 (2003) 4300.
- [34] J.A. Organero, L. Tormo, A. Douhal, *Chem. Phys. Lett.* 363 (2002) 409.
- [35] A. Douhal, M. Sanz, M.A. Carranza, J.A. Organero, L. Santos, *Chem. Phys. Lett.* 394 (2004) 54.
- [36] A. Shavel, N. Gaponik, A. Eychmuller, *J. Phys. Chem. B* 110 (2006) 19280.
- [37] Z. Tang, B. Ozturk, Y. Wang, N.A. Kotov, *J. Phys. Chem. B* 108 (2004) 6927.
- [38] M.G. Bawendi, W.L. Wilson, L. Rotherg, P.J. Carol, T.M. Jedju, M.L. Steigerwald, L.E. Brus, *Phys. Rev. Lett.* 65 (1990) 1623.
- [39] L.A. Padilha, A.A.R. Neves, C.L. Cesar, L.C. Barbosa, C.H. Brito Cruz, *Appl. Phys. Lett.* 85 (2004) 3256.
- [40] X. Ai, R. Jin, C. Ge, J. Wang, Y. Zou, X. Zhou, X. Xiao, *J. Chem. Phys.* 106 (1997) 3387.

- [41] M.A. El-Sayed, *Acc. Chem. Res.* 37 (2004) 326.
- [42] S.K. Pozniak, N.P. Osipovich, A. Shavel, D.V. Talapin, M. Gao, A. Eychemüller, N. Gaponik, *J. Phys. Chem. B* 109 (2005) 1094.
- [43] S. Xu, A.A. Mikhailovsky, J.A. Hollinsworth, V.I. Klimov, *Phys. Rev. B* 65 (2002) 045319.
- [44] T. Uchihara, H. Kato, E. Miyagi, *J. Photochem. Photobiol. A: Chem.* 181 (2006) 86.
- [45] M. Okamura, K. Ebina, S. Akimoto, I. Yamazaki, K. Uosaki, *J. Photochem. Photobiol. A: Chem.* 178 (2006) 156.
- [46] F. Wu, J.W. Lewis, D.S. Klinger, J.Z. Zhang, *J. Chem. Phys.* 118 (2003) 12.
- [47] Y. Wang, Z. Tang, M.A. Correa-Duarte, I. Pastoriza-Santos, M. Giersig, N.A. Kotov, L.M. Liz-Marzan, *J. Phys. Chem. B* 108 (2004) 15461.
- [48] J.Z. Zhang, *Acc. Chem. Res.* 30 (1997) 423.